IEEE Access
Multidisciplinary ⋮ Rapid Review ⋮ Open Access Journal

Received February 1, 2019, accepted February 15, 2019, date of publication March 14, 2019, date of current version April 13, 2019.

Digital Object Identifier 10.1109/ACCESS.2019.2901899

Sliding Mode Control for a Surgical Teleoperation System via a Disturbance Observer

SHUANG HAO[1], LINGYAN HU[1], AND PETER X. LIU[1,2], (Fellow, IEEE)
[1]School of Information and Engineering, Nanchang University, Nanchang 330031, China
[2]Department of Systems and Computer Engineering, Carleton University, Ottawa, ON K1S 5B6, Canada

Corresponding author: Lingyan Hu (hulingyan@ncu.edu.cn)

This work was supported in part by the National Natural Science Foundation of China under Grant 61563035, Grant 81501560, Grant 61662044, and Grant 61663027, in part by the Science and Technology Department of Jiangxi Province of China under Grant 20171BCB23008, in part by the Hundred People Voyage Funds from Jiangxi Science and Technology Association, and in part by the Postgraduate Innovation Fund of Jiangxi Province of China under Grant YC2018-S070.

ABSTRACT To obtain accurate trajectory tracking with robustness and faithful force feedback in a practical application, a sliding mode controller (SMC) combined with a compensation controller based on a nonlinear disturbance observer (DOB) is proposed. The DOB estimates the disturbances arising mainly from the uncertain dynamic model of a surgical manipulator, frictional forces and external interaction forces, and compensates for these disturbances in the control law. Accordingly, it alleviates the chattering problem caused by the SMC and improves tracking performance. The surgical teleoperation system using the proposed SMC-DOB is proved to be asymptotically stable using Lyapunov theory. The simulation and experiment results show that the surgical manipulator with the SMC-DOB can better track the trajectory of the master even in the presence of disturbances and the interaction forces between the instrument and the patient's tissues are faithfully presented to the surgeon.

INDEX TERMS Networked control system, surgical teleoperation system, disturbance observer, sliding mode control.

I. INTRODUCTION

Surgical robots have become widely used because they combine the knowledge and skills of the surgeon with the precision of a robot, thus enabling better treatment results [1]–[4]. The Da Vinci Surgical Robot is the most advanced surgical robot currently available. It is a human-centered robot, which means that it cannot act on its own initiative, but is completely controlled by the surgeon at the master side. During an operation, the surgeon controls a master haptic manipulator at the master side, and the position and velocity of this master manipulator are transmitted to the slave side as commands to the surgical robot through appropriate communication channels. The surgical robot at the slave side tracks the command trajectory from the master manipulator. The surgeon can observe a video of the operating procedure in real time. Meanwhile, the interaction force between the surgical manipulator and the patient's tissues at the slave side is transmitted back to the master side and presented to the surgeon in order to enhance his/her immersion. Ideally, the surgeon at the master side should be able to feel the interaction force from the slave side as if he/she were operating on the patient directly with traditional instruments. There has been some research into tactile aspects of robotic surgical systems [5]–[7].

Normally, the master and slave sides are located in the same room or in neighboring rooms [4]. When the distance between the master and slave sides becomes greater than this (for example, if they are in different cities), the master–slave system becomes a teleoperation surgical system. However, a time delay is inherent to such systems, and the greater this delay, the poorer is the system's performance. The reason for this degradation of performance is that a delay in force feedback may turn a negative feedback into a positive one, leading to system instability.

Many methods have been developed to solve the problem of instability in teleoperation systems caused by time delay and incorrect force feedback. Passive methods offer a credible approach to solve stability problems for teleoperation systems [8]. Since passivity is a sufficient condition for stability,

The associate editor coordinating the review of this manuscript and approving it for publication was Yanzheng Zhu.

much force fidelity is sacrificed, although this is actually not necessary to ensure system stability. In [9], a robust controller design method was developed for a class of NCSs with MCCs that are subject to channel switching governed by A Markov chain. Communication delays, packet dropouts and parameter uncertainties have been taken into account within a unified framework. Literature [10] has addressed the H_∞ filtering problem for discrete-time Markov jump LPV systems with both packet dropouts and channel noises in the networked scenario. Literature [11] developed a distributed state estimation method based on MHE for a class of two-time-scale nonlinear systems. These works have contributed to the teleoperation system based on network communication which enhanced robustness of the networked control system.

Advanced controllers, including sliding mode controllers (SMCs) and adaptive controllers, have recently been developed for teleoperation systems in order to obtain accurate trajectory tracking and faithful force feedback. One sliding mode approach, the three-mode control scheme, can implehent a position–position, force–force, or force–position scheme, and the results show good trajectory tracking perforhance [12]. However, it does not consider time delay. To solve the problem of the adverse effects of parametric uncertainties, an adaptive sliding mode control scheme was proposed by Motamedi *et al.* [13]. The algorithm has been verified on a teleoperation system with a single degree of freedom (DOF). Yang and Hua [14] proposed a novel nonsingular fast integral terminal sliding mode (NFITSM) for a teleoperation system, and practical experiments on one-DOF motion tracking have now been completed. A nonsingular terminal sliding mode and adaptive finite-time control method was proposed by Zhang *et al.* [15], and simulation results have verified the effectiveness of this method. These methods are useful attempts to design feedback controllers that improve the performance and stability of a teleoperation system.

Methods based on a disturbance observer (DOB) are a different type of control scheme. These are feedback/forward control methods that, through an observer, estimate the model errors and the external and internal disturbances, and then compensate for these errors and disturbances in the control law in order to improve performance. Such methods have been widely applied in control and robot systems. Chen *et al.* [16] and Nikoobin and Haghighi [17] designed nonlinear disturbance observers for planar serial manipulators with revolute joints. Mohahhadi *et al.* [18] developed a general systematic approach to solve the disturbance observer design problems presented in [16] and [17]. Recently, DOB-based approaches have been applied to bilateral teleoperation systems. Aboutalebian *et al.* [19] proposed a nonlinear DOB-based method with adaptive control for teleoperation systems in order to solve tracking problems using a dynamic model of the manipulators and taking account of environmental and operating forces. Simulations have shown that the system has good tracking performance. Chen *et al.* [20] developed an SMC with force compensation using a DOB for a teleoperation system without a force sensor. The observer estimates the environment force, and the force are fed forward to the SMC as compensation control. Meanwhile, the observer estimates the environmental parameters, which are transmitted to the master side to estimate the environmental force.

For a practical surgical teleoperation system, (i) the slave surgical manipulator should track the master accurately and quickly and (ii) the interaction force should be transmitted to the master and presented to the operator faithfully. To achieve these aims, we propose an SMC combined with a compensation controller based on a nonlinear DOB for a teleoperation system with force sensor. We call this integrated controller an SMC-DOB. The force sensor can measure the interaction forces between surgical instruments and patients' tissues, and these forces can be presented faithfully to the operator. The SMC controller is a feedback controller. It can endow system with robustness in the presence of bounded disturbances and uncertainties. However the sliding gain must be chosen to be bigger than the upper bound value of the lumped disturbances and large sliding gain causes large chattering in the system. The DOB is designed as a feedforward controller. It estimates lumped disturbances, which are principally uncertain dynamic model of manipulators, internal frictional forces and external interaction forces and compensates for these disturbances in the control law. To alleviate the chattering problem without sacrificing it's robustness, the composite controller SMC-DOB is proposed which combines the SMC feedback with the DOB based-feedforward compensation. The SMC-DOB thus ensures that the surgical manipulator accurately tracks the trajectory of the master with smaller chattering even in the presence of uncertain dynamic model of manipulators, internal frictional forces, and disturbances due to external interaction forces. The SMC-DOB has been applied to an actual surgical teleoperation system with six DOFs in the presence of time-varying delays. The surgical instrument, as the end-effector of the surgical manipulator, is able to track the command trajectory from the surgeon at the master side accurately and quickly, and the interaction force between the instrument and the patient's tissues can be presented faithfully to the surgeon.

The remainder of the paper is structured as follows: Section II describes the details of the SMC-DOB algorithm. The stability of the system is analyzed through Lyapunov theory in Section III. Simulation results are presented in Section IV. Experimental results are presented in Section V. Section VI gives the conclusions of the paper.

II. THE CONTROL SCHEME

In order to deal with the adverse effects of external disturbances and the surgical manipulator's dynamic uncertainties, we have developed a SMC-DOB for a 6-DOF surgical teleoperation system. The trajectory of the master manipulator is transmitted to the surgical manipulator as a command signal via a network with time delay. The controller developed in this paper is comprised by two parts: an SMC and a DOB. The SMC is a feedback controller to ensure that the

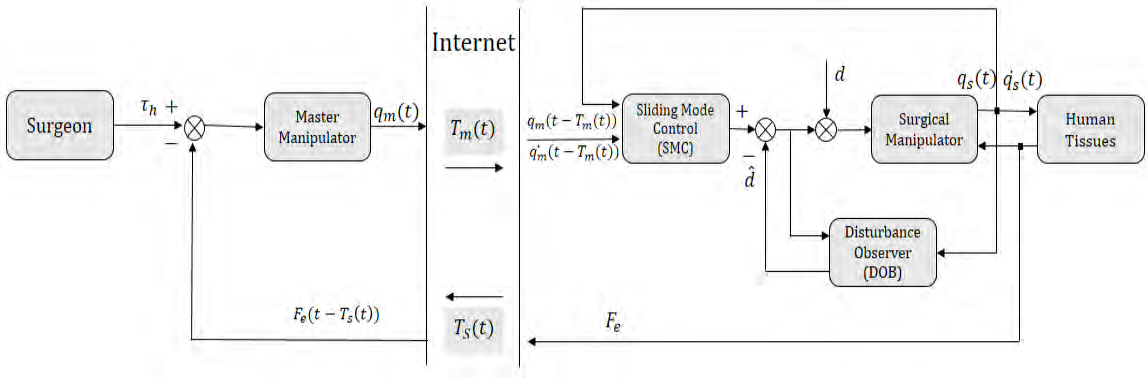

FIGURE 1. Control block diagram of the teleoperation system with SMC-DOB.

surgical manipulator tracks the master trajectory. The DOB is a feedforward controller that estimates lumped disturbances, including dynamic model uncertainties, friction, and external disturbances (mainly interaction forces), and then compensate for these disturbances in the control law. At the same time, the interaction force between the instrument and tissues is measured and transmitted faithfully to the surgeon. The surgical teleoperation system with the SMC-DOB is shown in Fig. 1.

Notation: For a n-dimensional vector $x = [x_1, x_2, ..., x_n]^T$, $x_i(i = 1, 2, ...n)$ represents the t-th element of x. The $sgn(x) = [sign(x_1), sign(x_2), ..., sign(x_n)]^T$. $\lambda_{max}(\cdot)$ and $\lambda_{min}(\cdot)$ denote the maximum and minimum eigenvalues of a matrix, respectively. The symbol $\|\cdot\|_1$ represents the 1-norm or its induced norm which is defined as $\|x\| = \sum_{i=1}^{n} |x_i|$ for a vector x. The symbol $\|\cdot\|$ represents the 2-norm or its induced norm which is defined as $\|x\| = \sqrt{x^T x}$ for a vector x and $\|A\| = \sqrt{\lambda_{max}(A^T A)}$ for a matrix A.

Assumption 1: The time-varying delays $T_m(t)$ and $T_s(t)$ are assumed to have the upper and lower bound and satisfy: $0 < T_m(t) = T_s(t) < T$, where T is a positive constant, $T_s(t)$ is the network time delay from the surgical manipulator to the master manipulator and $T_m(t)$ is the network time delay from the master manipulator to the surgical manipulator.

According to [21] and [22], the dynamic model of a surgical teleoperation system with n-DOFs can be expressed as:

$$\begin{cases} M_m(q_m)\ddot{q}_m + C_m(q_m, \dot{q}_m)\dot{q}_m + G_m(q_m) + F_m(q_m, \dot{q}_m) \\ = \tau_h - J_m^T F_e(t - T_s(t)), \\ M_s(q_s)\ddot{q}_s + C_s(q_s, \dot{q}_s)\dot{q}_s + G_s(q_s) + F_s(q_s, \dot{q}_s) \\ = \tau_s + J_s^T F_e, \end{cases} \tag{1}$$

where subscript m, s represent the master and the surgical manipulators, respectively, $q_m(t), q_s(t) \in \Re^n$ is the vector of joint displacements, $\dot{q}_m(t), \dot{q}_s(t) \in \Re^n$ is the joint velocity, $\ddot{q}_m(t), \ddot{q}_s(t) \in \Re^n$ is the joint acceleration, $M_m(q_m), M_s(q_s) : \Re^n \times \Re^n \to \Re^{n\times n}$ is the centrifugal force matrix, $C_m(q_m, \dot{q}_m), C_s(q_s, \dot{q}_s) : \Re^n \times \Re^n \to \Re^{n\times n}$ is the Coriolis force matrix, $G_m(q_m), G_s(q_s) : \Re^n \to \Re^n$ is the gravity matrix, and $F_m(q_m), F_s(q_s) : \Re^n \to \Re^n$ denote the friction torque vectors; $F_e \in \Re^n$ is the remote environmental forces, respectively, J_m, J_s is the Jacobian matrix, τ_h is the control torque of the master manipulator applied by the human operator, τ_s is the control torque of the surgical manipulator.

Remark 1: Force feedback is widely presumed to enhance performance in robotic surgery. References [23] and [24], Different from synchronization control for teleoperation systems recently that a controller is applied to the master manipulator [15], [25], [26], remote environment force F_e measured by the force sensor is transmitted to the master manipulator. The master manipulator is controlled by the surgeon directly. This ensure the surgeon in a telesurgery can feel the interaction force between surgical instruments and human tissues faithfully in the master side.

Property 1 [27]: $\dot{M}(q) - 2C(q, \dot{q})$ is a skew-symmetric matrix:

$$\zeta^T[\dot{M}(q) - 2C(q, \dot{q})]\zeta = 0 \quad \forall \zeta \in \Re^n. \tag{2}$$

Property 2 [27]: The inertia matrix $M(q)$ is symmetric and positive definite and satisfies:

$$\gamma_1 = \lambda_{min}(M(q)) \leqslant \|M(q)\| \leqslant \lambda_{max}(M(q)) = \gamma_2 \tag{3}$$

where γ_1,γ_2 are positive constants.

In practical experiments, it is very difficult to get the exact values of manipulator dynamic models' parameters. In this case, uncertain dynamic parts are introduced into the description of master and slave manipulator models. For $i = m, s$, we have

$$\begin{aligned} M_i(q_i) &= M_{oi}(q_i) + \Delta M_i(q_i) \\ C_i(q_i, \dot{q}_i) &= C_{oi}(q_i, \dot{q}_i) + \Delta C_i(q_i, \dot{q}_i) \\ G_i(q_i) &= G_{oi}(q_i) + \Delta G_i(q_i) \end{aligned} \tag{4}$$

where $M_{oi}(q_i)$, $C_{oi}(q_i, \dot{q}_i)$, and $G_{oi}(q_i)$ are the nominal parts in dynamic models; $\Delta M_i(q_i)$, $\Delta C_i(q_i, \dot{q}_i)$ and $\Delta G_i(q_i)$ are the uncertain parts. Friction also exists in practical experiments.

Therefore, the dynamic model of teleoperation system(1) can be rewritten as follows:

$$\begin{cases} M_{om}(q_m)\ddot{q}_m + C_{om}(q_m, \dot{q}_m)\dot{q}_m + G_{om}(q_m) \\ = \tau_h - J_m^T F_e(t - T_s(t)) + H_m(q_m, \dot{q}_m, \ddot{q}_m) - F_m(q_m, \dot{q}_s) \\ M_{os}(q_s)\ddot{q}_s + C_{os}(q_s, \dot{q}_s)\dot{q}_s + G_{os}(q_s) = \tau_s + d \end{cases} \tag{5}$$

where $H_m(q_m, \dot{q}_m, \ddot{q}_m)$ is the uncertainties of the master manipulator's dynamic model, d is defined as:

$$d = J_s^T F_e + H_s(q_s, \dot{q}_s, \ddot{q}_s) - F_s(q_s, \dot{q}_s), \tag{6}$$

where $H_s(q_s, \dot{q}_s, \ddot{q}_s)$ is the uncertainties of the surgical manipulator. d is the lumped disturbances of the surgical manipulator.

A. THE SMC CONTROLLER

We define the joint position errors of the surgical manipulator as

$$e_s = q_s - q_m(t - T_m(t)) \tag{7}$$

The sliding surface is defined as

$$S_s = \dot{e}_s + \Lambda e_s, \tag{8}$$

where $\Lambda = diag(c_1, c_2, \cdots c_i)$, $c_i > 0$.

We introduce a variable $\dot{q}_{sr} = \dot{q}_s - S_s$ and obtain

$$\begin{aligned} \dot{q}_{sr} &= \dot{q}_m(t - T_m(t)) - \Lambda e_s \\ \ddot{q}_{sr} &= \ddot{q}_m(t - T_m(t)) - \Lambda \dot{e}_s \end{aligned} \tag{9}$$

The SMC which can keep the system asymptotic stable without a compensation controller is designed as

$$\tau_{smc} = M_{os}(q_s)\ddot{q}_{sr} + C_{os}(q_s, \dot{q}_s)\dot{q}_{sr} + G_{os}(q_s) - \beta \operatorname{sgn}(S_s) \tag{10}$$

where β is the sliding gain which satisfies $\beta = \|d\| + \delta$, $\delta > 0$.

B. THE DISTURBANCE OBSERVER

The DOB is designed to estimate the lumped disturbances of the surgical manipulator, and then becomes part of the feedback control input. Before presenting specific design description of the DOB, the following assumption is introduced.

Assumption 2: The rate of change of the disturbances has a upper bounded which satisfies $\|\dot{d}\| \leqslant \alpha$ for all $t > 0$.

where α is a positive constants.

The DOB is represented as follows [16], [18]:

$$\begin{cases} \dot{z} = L(q_s)(C_{os}(q_s, \dot{q}_s)\dot{q}_s + G_{os}(q_s) - \tau_s) - L(q_s)\hat{d}, \\ \hat{d} = z + p(\dot{q}_s), \end{cases} \tag{11}$$

where $\hat{d}$, z, $p(\dot{q}_s)$, and $L(q_s)$ are respectively the estimate of the disturbances, the internal state of the nonlinear observer, the DOB auxiliary vector, and the DOB gain matrix that is to be designed.

The following DOB gain matrix and auxiliary vector are proposed:

$$L(q_s) = X^{-1} M_{os}(q_s)^{-1}, \tag{12}$$

$$p(\dot{q}_s) = X^{-1}\dot{q}_s, \tag{13}$$

where X is a constant invertible $n \times n$ matrix to be determined.

C. THE COMPOSITE CONTROLLER

In practical application of the teleoperation surgical teleoperation system, the interaction forces between surgical instruments and tissues which is external disturbances affects tracking performance of the surgical manipulator and stability of the system. To guarantee the stability of the system, the sliding gain β which we can get in (10) must be chosen to be bigger than the upper bound value of the lumped disturbances. But large sliding gain causes large chattering in the system. To alleviate the chattering problem without sacrificing the robustness, the composite controller SMC-DOB is proposed.

The composite controller is designed as follows:

$$\tau_s = M_{os}(q_s)\ddot{q}_{sr} + C_{os}(q_s, \dot{q}_s)\dot{q}_{sr} + G_{os}(q_s) - \delta \operatorname{sgn}(S_s) - \hat{d}. \tag{14}$$

where $\delta > 0$ is a small constant value which satisfies $\delta > \|d - \hat{d}\|$.

The DOB compensates the lumped disturbances of the surgical manipulator in the control law. Therefore the switching gain is greatly reduced so that the chattering problem is alleviated obviously.

III. STABILITY ANALYSIS

The stability of the surgical teleoperation system is analyzed through Lyapunov theory. To make the stability analysis clearer, the analysis is divided into three following steps. The first step proves the asymptotic stability of the master manipulator., the second step proves the observation error of the DOB is globally uniformly ultimately bounded, and the third step proves the asymptotic stability of the surgical manipulator.

Step 1:

Assumption 3: The surgeon is an SMC controller which controls the master manipulator and gives the command signals to the surgical manipulator.

In the master side, the master manipulator is completely controlled by the surgeon. Under this circumstance, the surgeon can be considered as a controller. In fact, surgeons have better intelligence and stronger robustness than general controllers. Therefore, to analyze the stability of the master side, it is reasonable to assume that the surgeon is a sliding mode controller.

Assumption 4: The force between the tissue and the instrument is bounded, which satisfies $0 \leqslant J_m^T F_e(t - T_s(t)) < \tau_h$.

We define the joint position errors of the master manipulator as

$$e_m = q_m - q_{md} \tag{15}$$

where q_{md} is the desired position of the master manipulator.

The sliding surface is defined as

$$S_m = \dot{e}_m + Ke_m, \tag{16}$$

where $K = diag(k_1, k_2, \cdots k_i)$, $k_i > 0$. The control torque of the master input by the surgeon is defined as

$$\tau_h = M_{om}(q_m)(\ddot{q}_d + K\dot{e}_m) + C_{om}(q_m, \dot{q}_m)(\dot{q}_m + Ke_m) + G_{om} + \xi \mathrm{sgn}(S_m). \tag{17}$$

where ξ a positive number.

Then we will prove the stability of the master manipulator. The positive definite Lyapunov function along the master side is proposed as:

$$V_1 = \frac{1}{2} S_m^T M_{om}(q_m) S_m \tag{18}$$

According to (5) (17) and Property 1, the time derivative of (18) is given by

$$\begin{aligned}\dot{V}_1 &= \frac{1}{2} S_m^T \dot{M}_{om}(q_m) S_m + S_m^T M_{om}(q_m)\dot{S}_m \\ &= S_m^T(-C_{om}(q_m, \dot{q}_m) - \xi \mathrm{sgn}(S_m) + J_m^T F_e(t - T_s(t)) \\ &\quad - H_m(q_m, \dot{q}_m, \ddot{q}_m) + F_m(q_m, \dot{q}_s) + \frac{1}{2} S_m^T \dot{M}_{om}(q_m) S_m \\ &= -\xi \|S_m\| - S_s^T J_m^T F_e(t - T_s(t)) - H_m(q_m, \dot{q}_m, \ddot{q}_m) \\ &\quad + F_m(q_m, \dot{q}_s) + \frac{1}{2} S_m^T (\dot{M}_{om}(q_m) - 2C_{om}(q_m, \dot{q}_m)) S_m \\ &= -\xi \|S_m\|_1 - S_m^T [J_m^T F_e(t - T_s(t)) - H_m(q_m, \dot{q}_m, \ddot{q}_m) \\ &\quad + F_m(q_m, \dot{q}_s)]\end{aligned} \tag{19}$$

According to *Assumption 4*, the remote environmental forces transmitted to the master side are bounded, there exists a positive number ξ satisfying

$$\xi > \|J_m^T F_e(t - T_s(t)) - H_m(q_m, \dot{q}_m, \ddot{q}_m) + F_m(q_m, \dot{q}_s)\| \tag{20}$$

We can get

$$\dot{V}_1 < 0 \tag{21}$$

Therefore we can get the master manipulator is asymptotic stability.

Step 2: Then the error between the output torque of the disturbance observer and the actual disturbance torque is defined as

$$e_{\mathrm{dob}} = d - \hat{d} \tag{22}$$

Consider the following candidate positive definite Lyapunov function:

$$V_2 = e_{\mathrm{dob}}^T X^T M_{os}(q_s) X e_{\mathrm{dob}} \tag{23}$$

According to Property 2, we can get that

$$\begin{aligned}\lambda_{max}(X^T M_{os}(q_s) X) &= \|(X^T M_{os}(q_s) X)\| \\ &\leqslant \|X^T\| \cdot \|M_{os}(q_s)\| \cdot \|X\| \\ &= \|M_{os}(q_s)\| \cdot \|X\|^2\end{aligned} \tag{24}$$

Therefore,

$$V_2 \leqslant \|M_{os}(q_s)\| \cdot \|X\|^2 \cdot \|e_{dob}\|^2 \tag{25}$$

According to Property 2, we can get that

$$V_2 \leqslant \gamma_2 \|X\|^2 \cdot \|e_{dob}\|^2 \tag{26}$$

$$V_2 \geqslant \gamma_1 e_{dob}^T X^T X e_{dob} \geqslant \gamma_1 \lambda_{min}(X^T X) \|e_{dob}\|^2 \tag{27}$$

According to (26) (27),

$$\gamma_1 \lambda_{min}(X^T X) \|e_{dob}\|^2 \leqslant V_2 \leqslant \gamma_2 \|X\|^2 \cdot \|e_{dob}\|^2 \tag{28}$$

From (11)–(13),

$$\begin{aligned}\dot{e}_{\mathrm{dob}} &= \dot{d} - \dot{\hat{d}} \\ &= \dot{d} - L(q_s)[M_{os}(q_s)\ddot{q}_s + C_{os}(q_s, \dot{q}_s)\dot{q}_s + G_{os}(q_s) - \tau_s] \\ &\quad + L(q_s)\hat{d} \\ &= \dot{d} + L(q_s)(\hat{d} - d),\end{aligned} \tag{29}$$

Using (29) the time derivative of (23) is given by

$$\begin{aligned}\dot{V}_2 = &-e_{dob}^T [X + X^T - X^T \dot{M}_{os}(q_s) X] e_{dob} \\ &+ \dot{e}_{dob}^T X^T M_{os}(q_s) X e_{dob} + e_{dob}^T X^T M_{os}(q_{os}) X \dot{\hat{d}}\end{aligned} \tag{30}$$

According to Property 2 and *Assumption 2*. we can get

$$\dot{e}_{dob}^T X^T M_{os}(q_s) \leqslant \alpha \gamma_2 \|X\|^2 \|e_{dob}\| \tag{31}$$

We construct the following inequality:

$$X - X^T \dot{M}_{os}(q_s) X + X^T \geq \Gamma, \tag{32}$$

where Γ is a symmetric positive-definite matrix. The value of X can be calculated by using the LMI toolbox in MATLAB.

According to (29) (31),

$$\begin{aligned}\dot{V}_2 &\leqslant -\lambda_{min}(\Gamma)\|e_{dob}\|^2 + 2\alpha\gamma_2 \|X\|^2 \|e_{dob}\| \\ &= -(1-\theta)\lambda_{min}(\Gamma)\|e_{dob}\|^2 - \theta\lambda_{min}(\Gamma)\|e_{dob}\|^2 \\ &\quad + 2\alpha\gamma_2 \|X\|^2 \|e_{dob}\|\end{aligned} \tag{33}$$

where θ is positive constant and satisfies $0 < \theta < 1$.

We can get

$$\dot{V}_2 \leqslant -(1-\theta)\lambda_{min}(\Gamma)\|e_{dob}\|^2 < 0, \forall \|e_{dob}\| \geqslant \frac{2\alpha\gamma_2\|X\|^2}{\theta\lambda_{min}(\Gamma)} \tag{34}$$

Therefore, according to the uniform ultimate boundedness theorems [28], we can get that the observation error is globally uniformly ultimately bounded. e_{dob} converges to the ball with radius $\frac{2\alpha\gamma_2\|X\|^2}{\theta\lambda_{min}(\Gamma)}$.

Step 3: We define the joint position errors of the surgical manipulator as

$$e_s = q_s - q_m(t - T_m(t)) \tag{35}$$

According to (5), the time derivative of the sliding surface in (8) is given by

$$\begin{aligned}\dot{S}_s &= \ddot{e}_s + \Lambda \dot{e}_s \\ &= M_{os}(q_s)^{-1}(\tau_s - C_{os}(q_s, \dot{q}_s)\dot{q}_s - G_{os}(q_s) + d) - \ddot{q}_{sr}\end{aligned} \tag{36}$$

Consider the following candidate positive definite Lyapunov function:

$$V_3 = \frac{1}{2} S_s^T M_{os}(q_s) S_s \tag{37}$$

According to (5),(36) The time derivative of (37) is given by

$$\begin{aligned}\dot{V}_3 &= S_s^T M_{os}(q_s)\dot{S}_s + \frac{1}{2} S_s^T \dot{M}_{os}(q_s) S_s \\ &= S_s^T [-C_{os}(q_s, \dot{q}_s)\dot{q}_s S_s - \delta \mathrm{sgn}(S_s) + e_{\mathrm{dob}}] + \frac{1}{2} S_s^T \dot{M}_{os}(q_s) S_s \\ &= -\delta \|S_s\|_1 - S_s^T e_{\mathrm{dob}} + \frac{1}{2} S_s^T [\dot{M}_{os}(q_s) - 2C_{os}(q_s, \dot{q}_s)] S_s \\ &= -\delta \|S_s\|_1 - S_s^T e_{\mathrm{dob}} \end{aligned} \tag{38}$$

When the sliding gain δ satisfies

$$\delta > \|e_{\mathrm{dob}}\| \tag{39}$$

We can get $\dot{V}_3 < 0$.

Based on the analysis in the step 2, there exist $\delta > 0$ satisfies (39).

Therefore, the surgical manipulator is asymptotically stable if the switching gain δ in composite controller (14) is designed such that $\delta > \|e_{\mathrm{dob}}\|$.

Accordingly, for this surgical teleoperation system, a candidate Lyapunov function can be chosen as

$$V = V_1 + V_2 + V_3 > 0 \tag{40}$$

On certain conditions, we can get

$$\dot{V} = \dot{V}_1 + \dot{V}_1 + \dot{V}_3 < 0 \tag{41}$$

Based on the above analysis, we can get the surgical teleoperation system (5) satisfies $\lim_{t\to\infty} \|e_m(t)\| = 0$ and $\lim_{t\to\infty} \|e_s(t)\| = 0$. This implies that the system is asymptotically stable.

IV. SIMULATION

A. SIMULATION SETUP AND PARAMETER SELECTION

The simulation experiments to prove the proposed control scheme are described in this section. The simulation is completed with MATLAB software. The master and surgical manipulators in this system are considered to be the 2-DOF robot arms with revolute joints. The dynamic model of the master and surgical manipulators are given by

$$M_m = M_s = \begin{bmatrix} M_{11} & M_{12} \\ M_{21} & M_{22} \end{bmatrix} \tag{42}$$

$$C_m = C_s = \begin{bmatrix} C_{11} & C_{12} \\ C_{21} & C_{22} \end{bmatrix} \tag{43}$$

$$G_m = G_s = \begin{bmatrix} G_1 \\ G_2 \end{bmatrix} \tag{44}$$

with

$$\begin{aligned} M_{11} &= (m_1 + m_2) l_1^2 + m_2 l_2 (2 l_1 cosq_2 + l_2) \\ M_{12} &= M_{21} = m_2 l_2^2 + m_2 l_1 l_2 cosq_2 \\ M_{22} &= m_2 l_2^2 \\ C_{11} &= -m_2 l_1 l_2 \dot{q}_2 sinq_2 \\ C_{21} &= -m_2 l_1 l_2 (q_1 + \dot{q}_2) sinq_2 \\ C_{21} &= m_2 l_1 l_2 \dot{q}_1 sinq_2 \\ C_{22} &= 0 \\ G_1 &= (m_2 l_2 cos(q_1 + q_2) + (m_1 + m_2) l_1 cos(q_2)) g \\ G_2 &= m_2 l_2 cos(q_1 + q_2) g \end{aligned} \tag{45}$$

The parameters of the master and slave are summarized as follows: $m_1 = 10\mathrm{kg}$, $m_2 = 5\mathrm{kg}$, $l_1 = 0.7\mathrm{m}$, $l_2 = 0.5\mathrm{m}$, $g = 9.8\mathrm{m/s}^2$.

The initial joint positions are chosen as $q_m(0) = [0\ 0]^T$ (rad) and $q_s(0) = [0\ 0]^T$ (rad). The initial joint velocities are chosen as $\dot{q}_m(0) = [0\ 0]^T$ (rad/s) and $\dot{q}_s(0) = [0\ 0]^T$ (rad/s).

The operator's command signal to the two joints are $q_d = [0.5sin(t), 0.5sin(t)]^T$. In practice, the master manipulator is completely controlled by the operator, therefore we can get $q_d = q_m$.

The disturbances we set to simulate the model errors, friction and external interaction forces are as follows,

$$d = \begin{cases} sin(pi * t), & t < 10, \\ 5sin(pi * t), & t \geq 10, \end{cases} \tag{46}$$

where t is running time of simulation and the disturbances apply to joint 1 and joint 2 are equal.

To demonstrate the superiority of the SMC-DOB over the SMC, we performed three groups of teleoperation simulation experiments with the time-varying delay and the disturbances presented in (44). We assume $T_m(t) = T_s(t)$ which are shown as Fig. 2.

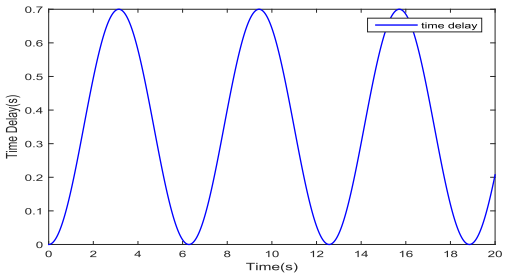

FIGURE 2. Forward and backward network time delay.

In the first experiment, the traditional SMC is applied in the system. The parameter of the SMC in (10) in the experiment was chosen as $\Lambda = \mathrm{diag}(150, 150)$, $\beta = 0.2$, which means the sliding gain $\beta < \|d\|$.

In the second experiment, the traditional SMC is applied in the system. The parameter of the SMC in (10) in the experiment was chosen as $\Lambda = \mathrm{diag}(150, 150)$, $\beta = 7$, which means the sliding gain $\beta > \|d\|$.

In the third experiment, the SMC-DOB is applied in the system. The parameter of the SMC-DOB in (14) in the experiment was chosen as $\Lambda = \mathrm{diag}(150, 150)$, $\delta = 0.2$, which means the sliding gain $\beta > \|e_{dob}\|$, and $X = [0.02 \quad 0, -0.02 \quad 0.02]^T$.

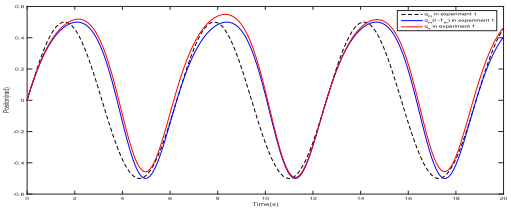

FIGURE 3. Trajectory tracking of joint 1 in experiment 1. ($\beta = 0.2$).

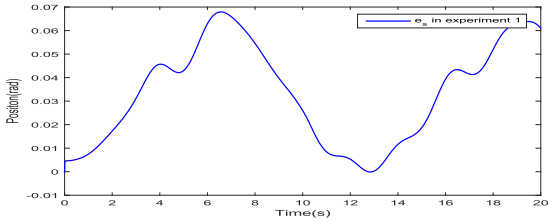

FIGURE 4. Tracking error of slave manipulator in experiment 1. ($\beta = 0.2$).

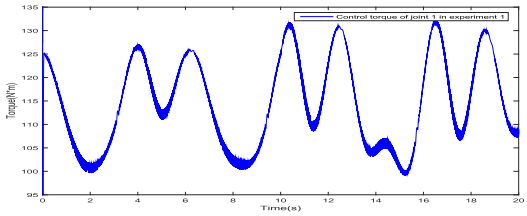

FIGURE 5. Control torque of joint 1 in experiment 1. ($\beta = 0.2$).

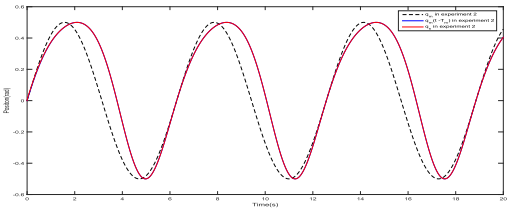

FIGURE 6. Trajectory tracking of joint 1 in experiment 2. ($\beta = 7$).

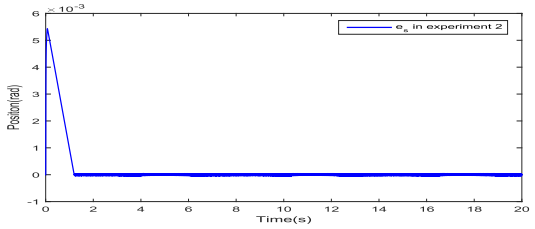

FIGURE 7. Tracking error of slave manipulator in experiment 2. ($\beta = 7$).

B. RESULTS AND DISCUSSION

For the sake of brevity, we only present the simulation results of Joint 1. In the three experiments, we applied the same disturbances which can be seen in (44) and Fig. 12. The results of the trajectory tracking and tracking error of the slave manipulator of the three groups of experiment are shown in Figs. 3, 4, 6, 7, 9 10. The control torques are shown in Figs. 5, 8, 11. The disturbances and the output of the DOB is shown in Fig. 12. The observation error of the DOB in experiment 3 is shown in Fig. 13.

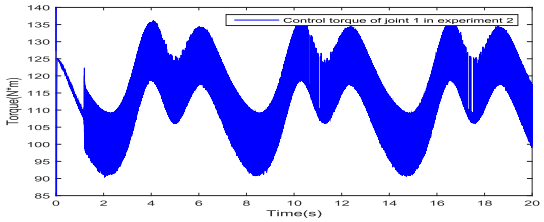

FIGURE 8. Control torque of joint 1 in experiment 2. ($\beta = 7$).

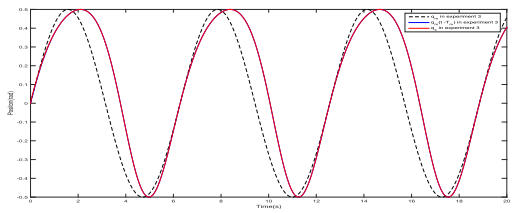

FIGURE 9. Trajectory tracking of joint 1 in experiment 3. ($\delta = 0.2$).

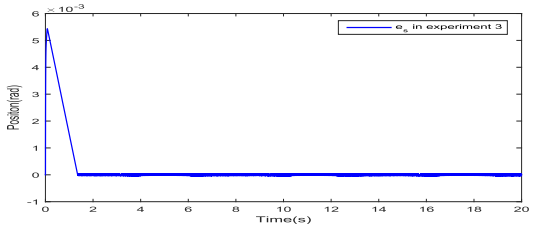

FIGURE 10. Tracking error of slave manipulator in experiment 3. ($\delta = 0.2$).

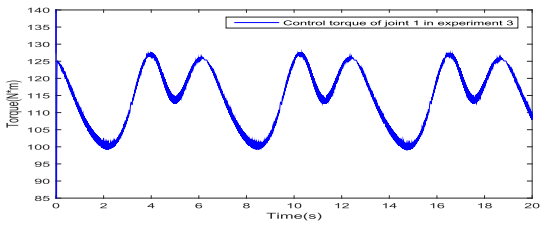

FIGURE 11. Control torque of joint 1 in experiment 3. ($\delta = 0.2$).

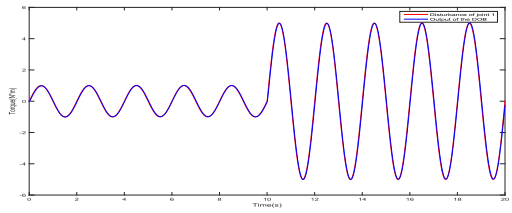

FIGURE 12. Disturbances and output of the DOB in experiment 3.

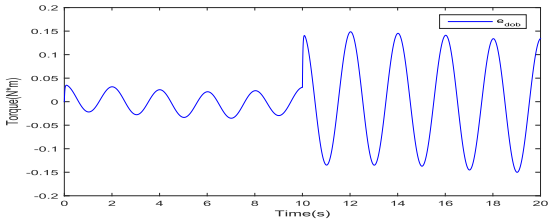

FIGURE 13. The observation error of the DOB in experiment 3.

In the experiment 1, the SMC with the sliding gain is $\beta = 0.2$ which satisfies $\beta < \|d\|$. The chattering of the control torque is small which is shown in Fig. 5. But the slave manipulator can't track the master well with the

disturbances and the convergence of tracking error can't be guaranteed. The trajectory tracking and tracking error are shown in Figs. 3, 4.

In the experiment 2, the sliding gain is increased which is $\beta = 7$ and satisfies $\beta > \|d\|$. When the sliding gain is bigger than the upper bound value of the lumped disturbances, the tracking error can converge to the minimal neighborhood of zero is shown in Fig. 7. However, the chattering of the control torque is shown in Fig. 8 which is much more than that in experiment 1. Because large sliding gain causes large high-frequency oscillations of the controller output. The chattering problem has negative impaction on the application of the SMC.

In the experiment 3, the sliding gain is $\delta = 0.2$ which satisfies $\delta > e_{dob}$. The tracking error with SMC-DOB can converge to the minimal neighborhood of zero is shown in Fig. 10. The control torque with small chattering is shown in Fig. 11. The DOB can estimate the lumped disturbances accurately which is shown in Fig. 12. The observation error is shown in Fig. 13. Compared with the traditional SMC experiment 1, the SMC-DOB in experiment 3 has better trajectory tracking performance and the tracking error is convergent. Compared with the SMC in experiment 2, the chattering problem has been obviously alleviated.

FIGURE 14. Teleoperation surgical system.

V. EXPERIMENT

A. EXPERIMENTAL SETUP AND PARAMETER SELECTION

A surgical teleoperation system (Fig. 14) is set up to verify the proposed SMC-DOB controller. A Phantom Premium 1.5 manipulator and a Denso manipulator are used as master manipulator and surgical manipulator, respectively. These manipulators are controlled by two computers and connected via the Internet. The time delay and other parameters of the network can be set in the control program. A six-dimensional force sensor is installed at the end of the surgical manipulator. A puncture needle, which serves as the surgical instrument, is attached beneath the force sensor. The control algorithm is implemented in MATLAB.

The surgeon performs telesurgery by controlling the master manipulator, the trajectory of which is transmitted to the slave side through the network as the command trajectory of the surgical manipulator. The surgical manipulator tracks the command trajectory from the master side with the SMC-DOB. As a result, the puncture needle interacts with the patient's tissues along the expected trajectory. The interaction force between the puncture needle and the tissues is transmitted back to the master, and presented faithfully to the surgeon.

The most important components of the overall performance of a surgical teleoperation system are trajectory tracking performance, force feedback fidelity, and robust stability. Therefore, the objective of the experiment is to verify that the surgical manipulator can track the trajectory of the master stably and quickly in the presence of time delay and disturbances, while simultaneously the interaction force is transmitted faithfully back to the master and presented faithfully to the surgeon.

For comparison, we performed two groups of teleoperation experiments with the SMC-DOB and the SMC, to verify their performances in the presence of different time delays. The first experiment was carried out with a 1 s time delay and the second with a time-varying time delay. For simplicity, we only moved two joints of the manipulators in these experiments.

To visualize the trajectory tracking, we recorded the master and slave positions at the slave side, so the master positions in all the figures presented here are $q_{mi} = q_{mi}(t - T_m(t))$, $i = 1, 2$, which are shifted back by a time delay $T_m(t)$. In all of the experiments, the interaction force between the puncture needle and tissue was measured by the force sensor and presented to the surgeon faithfully. To show the effectiveness of the DOB in alleviating the chattering problem caused by the SMC, we recorded the control current of the surgical manipulator. We then recorded the control currents of the SMC-DOB and SMC together after filtering to provide an appropriate comparison.

The initial joint positions were chosen as $q_m(0) = [0 \ -\pi/2]^T$ (rad) and $q_s(0) = [0 \ -\pi/2]^T$ (rad). The initial joint velocities are chosen as $\dot{q}_m(0) = [0\ 0]^T$ (rad/s) and $\dot{q}_s(0) = [0\ 0]^T$ (rad/s).

In practical applications, to minimize the damage of chattering to manipulator as much as possible, boundary layer method [29] is adopted in the experiments. We chose a saturation function instead of the sign function in the SMC. The saturation function is defined as

$$\text{sat}(S_s) = \begin{cases} 1, & S_s > \Delta, \\ kS_s, & |S_s| \le \Delta, \quad k = 1/\Delta, \\ -1, & S_s < -\Delta, \end{cases} \tag{47}$$

where Δ is the boundary-layer thickness.

The parameters of the SMC controller in (11) were chosen as $\Lambda = \text{diag}(5, 5)$, $\beta = 3$, and $\Delta = 0.2$.

The parameters of the SMC-DOB controller in (15) were chosen as $\Lambda = \text{diag}(5, 5)$, $\delta = 1.3$, $\Delta = 0.2$, $X = \text{diag}(3.2, 3.2)$.

B. RESULTS AND DISCUSSION

1) TELEOPERATION EXPERIMENTS WITH CONSTANT TIME DELAY

In the first group of experiments, the time delay between the master and surgical manipulator was set as 1 s. The surgeon

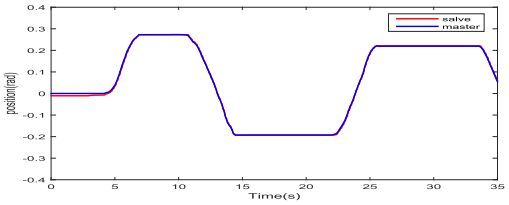

FIGURE 15. Position of joint 1 (SMC-DOB).

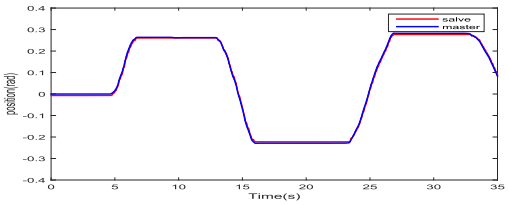

FIGURE 16. Position of joint 1 (SMC).

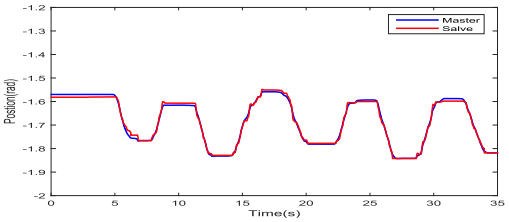

FIGURE 17. Position of joint 2 (SMC-DOB).

moved the master manipulator to control the surgical manipulator so that it moved its puncture needle into and out of soft tissue.

The positions and forces for the master and slave manipulators with the SMC-DOB and the SMC are shown in Figs. 15, 19, 22 and Figs. 17, 21, 23, respectively. Because the force feedback is same as the interaction force, we do not have to show the force along all three axes.

For simplicity, we show only the force along the z axis, which is the largest of the three. Both the surgical manipulator with the SMC-DOB and that with the SMC can track the trajectory of the master, with the interaction being transmitted to the master and presented to the operator without any change, as shown in Figs. 15, 17 and Figs. 16, 18. To provide a further comparison of the tracking performances of the SMC-DOB and the SMC, we calculated the average tracking errors of joints 1 and 2 from Figs. 15, 17 and Figs. 16, 18, and these are shown in Table 1. The average error of the SMC-DOB is much less than that of the SMC. The reason is that the DOB estimates the environmental force and other disturbances, and compensates for these in the control law. Thus, the tracking performance of the SMC-DOB is better than that of the SMC. Moreover, the DOB can alleviate the chattering problem caused by the SMC, because it is able to compensate for disturbances. The control currents of the surgical manipulator with the SMC-DOB and the DOB are shown in Fig. 16, from which it can be seen that the current chattering for the SMC-DOB is less than that for the SMC.

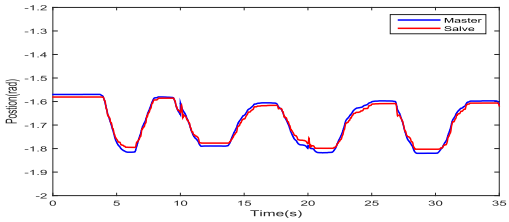

FIGURE 18. Position of joint 2 (SMC).

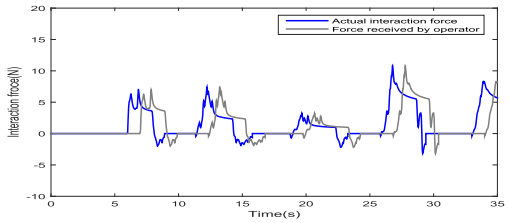

FIGURE 19. Force in the z direction (SMC-DOB).

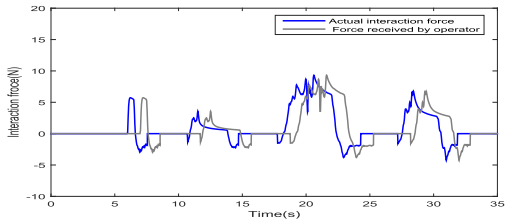

FIGURE 20. Force in the z direction (SMC).

TABLE 1. Average tracking error with constant time delay.

Average error	Joint 1	Joint 2
SMC-DOB	0.0029 rad	0.0058 rad
SMC	0.0052 rad	0.0117 rad

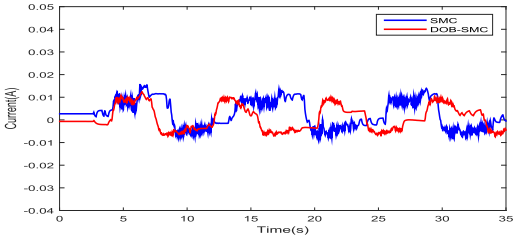

FIGURE 21. Comparison of the control current of joint 2 of the surgical manipulators with constant time delay.

2) TELEOPERATION EXPERIMENTS WITH TIME-VARYING TIME DELAY

In the second group of experiments, we repeated the previous teleoperation experiment, but with time-varying time delay. The time delay was set as follows:

$$T_m(t) = Ts(t) = \begin{cases} 0.6\,s, & 0\,s < t \le 10\,s, \\ 1\,s, & 10\,s < t \le 15\,s, \\ 1.2\,s, & 15\,s < t \le 25\,s, \\ 1\,s, & 25\,s < t \le 30\,s, \\ 0.6\,s, & 30\,s < t \le 40\,s. \end{cases}$$

The other parameters were the same as in the first group of experiments. The puncture needle moved into and out of the tissue as commanded.

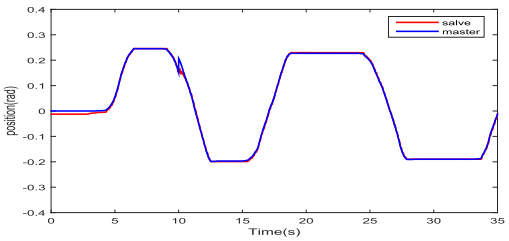

FIGURE 22. Position of joint 1 (SMC-DOB).

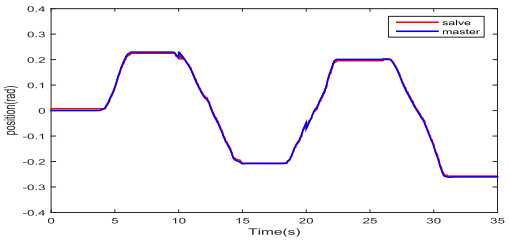

FIGURE 23. Position of joint 1 (SMC).

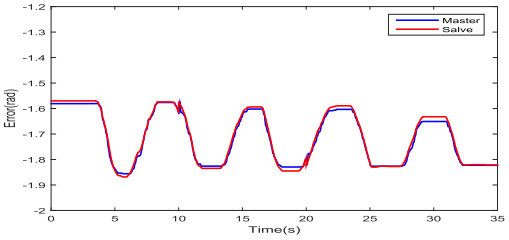

FIGURE 24. Position of joint 2 (SMC-DOB).

The positions and forces for the master and surgical manipulators with the SMC-DOB and the SMC are shown in Figs. 22, 24, 26 and Figs. 23, 25, 27, respectively. As can be seen from Figs. 22 and 24, the surgical manipulator with the SMC-DOB can track the trajectory of the master manipulator in the case of time-varying delay as well as in the case of constant delay, with the interaction force being presented to the operator without any change. In contrast, the surgical manipulator with the SMC cannot track the master so well, as shown in Figs. 23 and 25. The teleoperation system with the SMC-DOB exhibits better adaptability than that with the SMC, because the DOB is able to estimate and compensate for external and internal disturbances in an adaptive manner. Meanwhile, because the DOB compensates for disturbances in the control law, the control current of the SMC-DOB is subject to less chattering than that of the SMC. The control currents of the SMC-DOB and the SMC are shown in Fig. 28.

From the above two groups of experiments, we can conclude that the SMC-DOB is able to maintain the stability of a surgical teleoperation system in the presence of time-varying

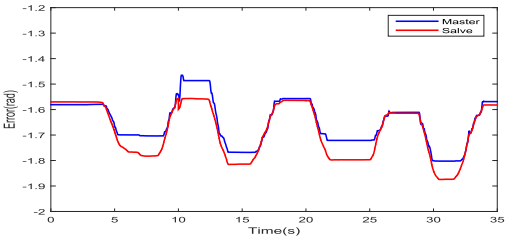

FIGURE 25. Position of joint 2 (SMC).

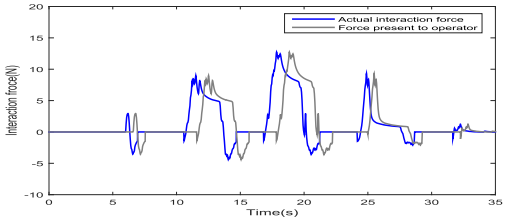

FIGURE 26. Force in the z direction (SMC-DOB).

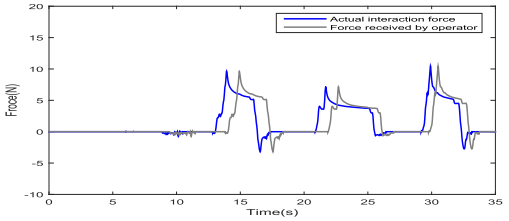

FIGURE 27. Force in the z direction (SMC).

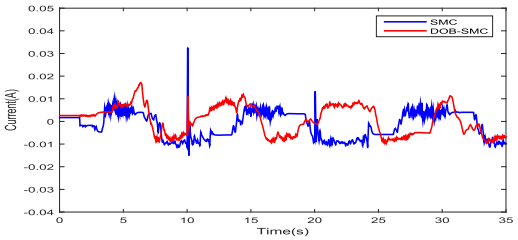

FIGURE 28. Comparison of the control current of joint 2 of the surgical manipulators with time-varying time delay.

time delay, with the interaction force being transmitted to the master and presented to the operator without any change, and thus the SMC-DOB can maintain system stability without sacrificing system fidelity. Moreover the system with the SMC-DOB has better trajectory tracking performance than the system with the SMC, because the DOB compensates for model uncertainties, internal and external disturbances in the control law.

VI. CONCLUSION

An SMC-DOB combining sliding mode control with disturbance observer feedforward control is proposed in this paper. The DOB based-feedforward compensation controller alleviates the chattering problem of the SMC while enhances robustness of the system. For the proposed SMC-DOB, simulation and experimental results show that the surgical manipulator with SMC-DOB can accurately track the trajectory of

the master with smaller chattering even in the presence of uncertain dynamic model of manipulators, internal frictional forces, and disturbances due to external interaction forces. The interaction force between the instrument and the patient's tissues can be faithfully presented to the surgeon.

REFERENCES

[1] O. Øyen, "Minimally invasive renal transplantation," in *Understanding the Complexities of Kidney Transplantation*. Rijeka, Croatia: InTech, 2011.

[2] G. A. Antoniou, C. V. Riga, E. K. Mayer, N. J. Cheshire, and C. D. Bicknell, "Clinical applications of robotic technology in vascular and endovascular surgery," *J. Vascular Surgery*, vol. 53, no. 2, pp. 493–499, Feb. 2011.

[3] S. Kalan *et al.*, "History of robotic surgery," *J. Robotic Surgery*, vol. 4, no. 3, pp. 141–147, Sep. 2010.

[4] S. Avgousti *et al.*, "Medical telerobotic systems: Current status and future trends," *Biomed. Eng. Online*, vol. 15, no. 1, p. 96, Aug. 2016.

[5] M. M. Dalvand, S. Nahavandi, M. Fielding, J. Mullins, Z. Najdovski, and R. D. Howe, "Modular instrument for a haptically-enabled robotic surgical system (herosurg)," *IEEE Access*, vol. 6, pp. 31974–31982, 2018.

[6] Y. Yang, H. Chen, Y. Lou, and W. Lin, "Remote master-slave control of a 6d manipulator for cardiac surgery application," in *Proc. IEEE Int. Conf. Robot. Biomimetics*, Dec. 2014, pp. 1799–1804.

[7] B. Willaert, J. Bohg, H. Van Brussel, and G. Niemeyer, "Towards multi-DOF model mediated teleoperation: Using vision to augment feedback," in *Proc. IEEE Symp. Haptic Audio-Visual Evironments Games*, Oct. 2012, pp. 25–31.

[8] R. Anderson and M. W. Spong, "Bilateral control of teleoperators with time delay," *IEEE Trans. Autom. Control*, vol. 34, no. 5, pp. 494–501, May 1989.

[9] X. Yin, L. Zhang, Y. Zhu, C. Wang, and Z. Li, "Robust control of Networked systems with variable communication capabilities and application to a semi-active suspension system," *IEEE/ASME Trans. Mechatron.*, vol. 21, no. 4, pp. 2097–2107, Aug. 2016.

[10] Y. Zhu, Z. Zhong, W. X. Zheng, and D. Zhou, "HMM-based $\mathcal{H}_\infty$ filtering for discrete-time Markov jump LPV systems over unreliable communication channels," *IEEE Trans. Syst., Man, Cybern. Syst.*, vol. 48, no. 12, pp. 2035–2046, Sep. 2017.

[11] X. Yin and J. Liu, "Distributed moving horizon state estimation of two-time-scale nonlinear systems," *Automatica*, vol. 79, pp. 152–161, May 2017.

[12] R. Moreau, M. T. Pham, M. Tavakoli, M. Le, and T. Redarce, "Sliding-mode bilateral teleoperation control design for master–slave pneumatic servo systems," *Control Eng. Pract.*, vol. 20, no. 6, pp. 584–597, Jun. 2012.

[13] M. Motamedi, M. T. Ahmadian, G. Vossoughi, S. M. Rezaei, and M. Zareinejad, "Adaptive sliding mode control of a piezo-actuated bilateral teleoperated micromanipulation system," *Precis. Eng.*, vol. 35, no. 2, pp. 309–317, Apr. 2011.

[14] Y. Yang, C. Hua, J. Li, and X. Guan, "Finite-time output-feedback synchronization control for bilateral teleoperation system via neural Networks," *Inf. Sci.*, vols. 406–407, pp. 216–233, Sep. 2017.

[15] H. Zhang, A. Song, and S. Shen, "Adaptive finite-time synchronization control for teleoperation system with varying time delays," *IEEE Access*, vol. 6, pp. 40940–40949, 2018.

[16] W.-H. Chen, D. J. Ballance, P. J. Gawthrop, and J. O'Reilly, "A nonlinear disturbance observer for robotic manipulators," *IEEE Trans. Ind. Electron.*, vol. 47, no. 4, pp. 932–938, Aug. 2000.

[17] A. Nikoobin and R. Haghighi, "Lyapunov-based nonlinear disturbance observer for serial n-link robot manipulators," *J. Intell. Robotic Syst.*, vol. 55, nos. 2–3, pp. 135–153, 2009.

[18] A. Mohammadi, M. Tavakoli, H. J. Marquez, and F. Hashemzadeh, "Nonlinear disturbance observer design for robotic manipulators," *Control Eng. Pract.*, vol. 21, no. 3, pp. 253–267, Mar. 2013.

[19] B. Aboutalebian, H. A. Talebi, and A. A. Suratgar, "Nonlinear disturbance observer based adaptive control for nonlinear teleoperation systems," in *Proc. 3rd RSI Int. Conf. Robot. Mechatron. (ICROM)*, 2015, pp. 091–095.

[20] Z. Chen, Y. J. Pan, and J. Gu, "Adaptive robust control of bilateral teleoperation systems with unmeasurable environmental force and arbitrary time delays," *IET Control Theory Appl.*, vol. 8, no. 15, pp. 1456–1464, Oct. 2014.

[21] I. G. Polushin, P. X. Liu, and C.-H. Lung, "A control scheme for stable force-reflecting teleoperation over IP networks," *IEEE Trans. Syst., Man, , Part B Cybern.*, vol. 36, no. 4, pp. 930–939, Aug. 2006.

[22] N. Chopra, M. W. Spong, R. Ortega, and N. E. Barabanov, "On tracking performance in bilateral teleoperation," *IEEE Trans. Robot.*, vol. 22, no. 4, pp. 861–866, Aug. 2006.

[23] C. R. Wagner, N. Stylopoulos, P. G. Jackson, and R. D. Howe, "The benefit of force feedback in surgery: Examination of blunt dissection," *Presence, Teleoper. Virtual Environ.*, vol. 16, no. 3, pp. 252–262, 2007.

[24] M. Mahvash *et al.*, "Force-feedback surgical teleoperator: Controller design and palpation experiments," in *Proc. Symp. Haptic Interfaces. Virtual Environ. Teleoperator Syst.*, Mar. 2008, pp. 1–9.

[25] Y. Yang, C. Hua, and X. Guan, "Finite time control design for bilateral teleoperation system with position synchronization error constrained," *IEEE Trans. Cybern.*, vol. 46, no. 3, pp. 609–619, Mar. 2016.

[26] D.-H. Zhai and Y. Xia, "Adaptive control for teleoperation system with varying time delays and input saturation constraints," *IEEE Trans. Ind. Electron.*, vol. 63, no. 11, pp. 6921–6929, Aug. 2016.

[27] M. W. Spong and M. Vidyasagar, *Robotics: Dynamics and Control*. Hoboken, NJ, USA: Wiley, 2008.

[28] H. K. Khalil and J. Grizzle, *Nonlinear System*, vol. 3. Upper Saddle River, NJ, USA: Prentice Hall, 2002.

[29] J.-J. E. Slotine *et al.*, *Applied Nonlinear Control*. Englewood Cliffs, NJ, USA: Prentice Hall, 1991.

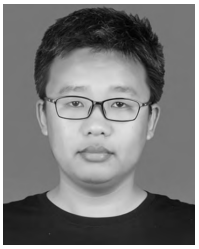

SHUANG HAO is currently pursuing the master's degree in automation with Nanchang University. His research interests include haptic manipulator control and teleoperation.

LINGYAN HU received the Ph.D. degree from Nanchang University, in 2011. She held a Post-Doctoral position at the Department of Systems and Computer Engineering, Carleton University, Ottawa, ON, Canada. She is currently a Professor with the School of Information Engineering, Nanchang University, Nanchang, China. Her current research interests include teleoperation systems, haptic control, and virtual surgery.

PETER X. LIU (F'19) received the B.Sc. and M.Sc. degrees from Northern Jiaotong University, Beijing, China, in 1992 and 1995, respectively, and the Ph.D. degree from the University of Alberta, Edmonton, AB, Canada, in 2002.

Since 2002, he has been with the Department of Systems and Computer Engineering, Carleton University, Ottawa, ON, Canada, where he is currently a Professor and the Canada Research Chair. He is currently an Adjunct Professor with Nanchang University. He has published over 250 research articles. His research interests include interactive networked systems and teleoperation, haptics, surgical simulation, robotics, intelligent systems, and context-aware systems.

Prof. Liu is a Licensed Member of the Professional Engineers of Ontario (P.Eng) and a Fellow of Engineering Institute of Canada. He is an Associate Editor of several journals including the IEEE/ASME TRANSACTIONS ON MECHATRONICS, the IEEE TRANSACTIONS ON CYBERNETICS, the IEEE TRANSACTIONS ON AUTOMATION SCIENCE AND ENGINEERING, and the IEEE ACCESS.